Acta Polytechnica **62**(6):607–617, 2022
https://doi.org/10.14311/AP.2022.62.0607

Published by the Czech Technical University in Prague

APPLICATION OF STRUT-AND-TIE MODELS FOR ASSESSING RC HALF-JOINTS NOT COMPLYING WITH CURRENT CODE SPECIFICATIONS

Gregoria Kotsovou[a], Emmanouil Vougioukas[b], Demetrios M. Cotsovos[c,*]

[a] *Independent consultant, Athens, Greece*

[b] *National Technical University of Athens (NTUA), Laboratory or Reinforced Concrete Structures, 5 Iroon Polytechniou, Zografou, Athens 15780, Greece*

[c] *Heriot-Watt University, Institute of Infrastructure and Environment, School of Energy, Geoscience, Infrastructure & Society, Edinburgh EH14 4AS, UK*

[*] corresponding author: D.Cotsovos@hw.ac.uk

Abstract.

The work described is concerned with an investigation of the effectiveness of the use of strut-and-tie models for the structural assessment of half joints. Such elements form a part of many existing bridges which, although not complying with current code specifications, have not as yet displayed any significant signs of distress in spite of the increase in traffic volume and loads over the years. The work is based on a comparative study of the predicted and experimentally established values of load-carrying capacity and location and causes of failure of half-jointed beams with reinforcement layouts that replicate those found in structures designed in accordance with previous code specifications. The results obtained show significant shortcomings of the assessment method as this is found not only to underestimate load-carrying capacity by a margin ranging between 40 % and 65 %, but also to often fail to identify the location and causes of failure. Therefore, there is a need for an alternative assessment method that will be based on concepts capable of both providing a realistic description of structural-concrete behaviour and identifying the causes of failure leading to the loss of load-carrying capacity.

Keywords: Half joint, reinforced concrete, structural assessment, strut-and-tie models.

1. Introduction

Strut-and-Tie Models (STMs) are widely used to describe the function of reinforced concrete (RC) members at their ultimate limit state (ULS). It is considered that through them, it is possible to obtain a realistic representation of the flow of internal stresses developing in the RC members during the transfer of the applied load to the supports [1]. This flow of internal stresses is assumed to form a triangulated, statically determinate truss and the forces in individual struts and ties can be calculated in a straightforward manner solely based on principles of equilibrium.

While designing new structures, the selection of appropriate STM geometry requires skill and understanding of the flow of stresses within a deformable solid; reinforcing bars are then selected so as to have the required strength and checks conducted to verify that a failure of the concrete struts cannot occur before the strength of the ties is exhausted. Transfer of forces between struts and ties must also be checked. Such a calculation approach is widely considered to be capable of producing design solutions that satisfy the requirements of current codes for structural performance, such as those of EC2 [2] and EC8 [3].

However, in recent years there has been an increasing need for the assessment of structures designed in accordance with past codes of practice as they do not conform with current design specifications and do not satisfy the corresponding requirements for structural performance. In spite these shortcommings many such structures have not displayed, to date, any significant sign of distress even in the case of existing bridges where there has been an increase in traffic volume and loads over the years. Nevertheless, the need for the available margin of safety to be realistically assessed remains. Therefore, a question arises: can STMs be as effective for the assessment of existing structures as they are considered to be for the design of new structures?

The work presented herein attempts to provide an answer to the above question through a comparative study of STM predictions and published experimental results on the behaviour of half-jointed RC beams with different arrangements of transverse reinforcement. The RC members assessed in the present work have been selected from the literature due to their practical significance as, in accordance with Transport Scotland [4], they are relevant to over 400 half-jointed concrete bridges in the UK Highways England network alone that do not comply with current design specifications.

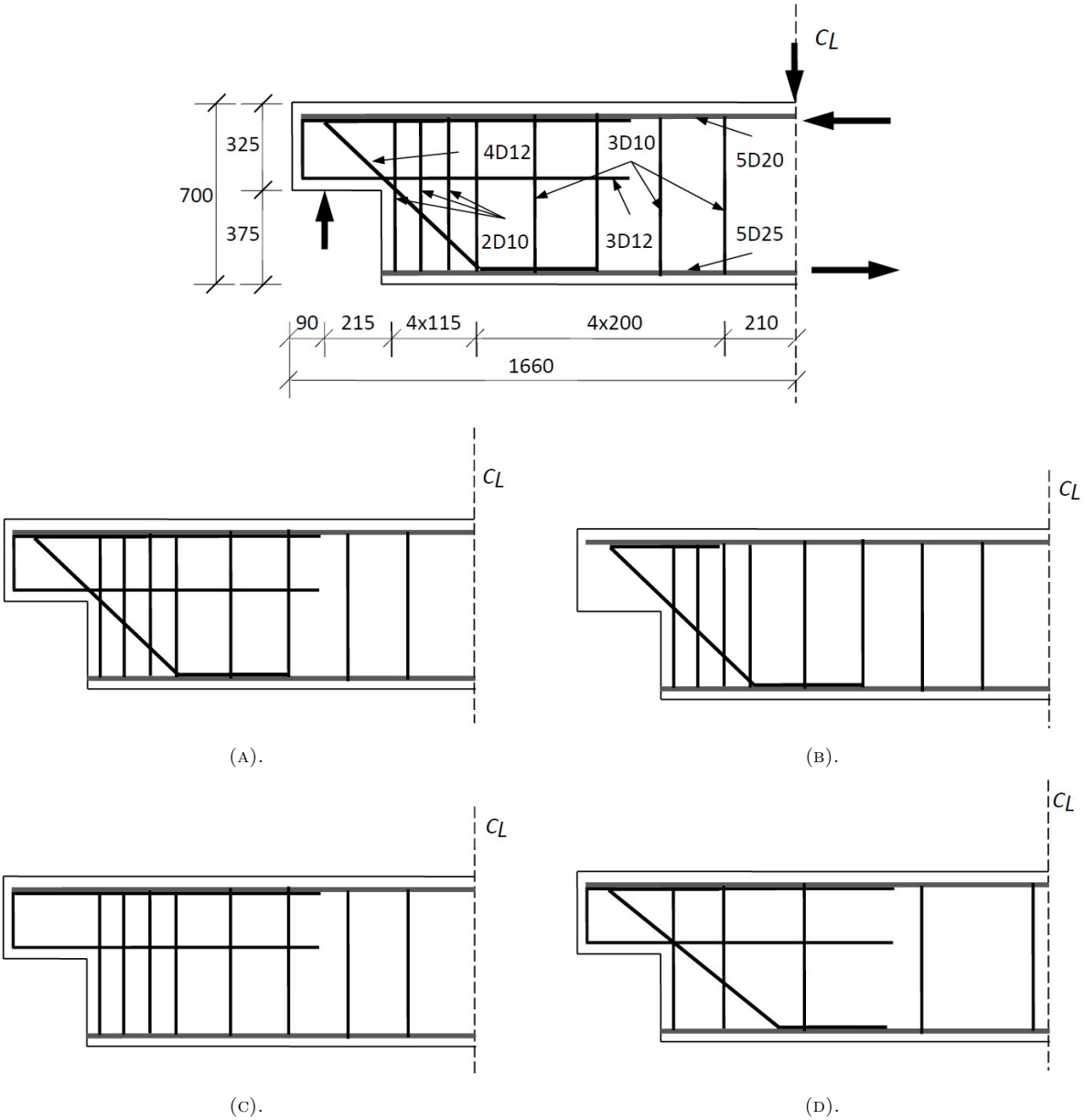

FIGURE 1. Top: Geometry, dimensions and reinforcement details of half-joint specimens. Bottom: Reinforcement layouts for the different test scenarios: (A) NS-REF, (B) NS-NU, (C) NS-ND, and (D) NS-RS.

2. HALF-JOINT BEAMS ASSESSED

The design details of the half-jointed beams used for investigating the suitability of STMs for a structural assessment are shown in Figure 1. These beams were tested under point loading (applied monotonically to failure) as described in [5], where a detailed description of the experimentally established behaviour of the specimens is presented. The uniaxial cylinder compressive strength of concrete at the time of testing was around 37 MPa and the yield stress of the steel reinforcement was 539 MPa and 529 MPa for the 10 mm and 12 mm diameter bars, respectively, and 578 MPa for the bars with a diameter of 20 mm or 25 mm.

Four different specimens were tested:

- One reference specimen, NS-REF, by considering the nib as the region with geometrical discontinuities (D-region) while the other regions of the beam are referred as beams or Bernoulli regions (B-regions). In the latter regions, the design was based on bending and shear theory and the Bernoulli assumption of "plane sections remain plane" is valid. In D-regions, due to the discontinuities, this assumption is not valid and the design was based on alternative methods such as strut-and-tie approaches [6].

- One specimen without the diagonal reinforcing bars, RS-ND, but where the reinforcement layout was otherwise identical to that of specimen NS-REF.

- One specimen without the U-bars, NS-NU, but also in all other aspects identical to specimen NS-REF, and, finally,
- One specimen identical to NS-REF in all aspects, but with a reduced number of shear links, NS-RS.

The three beams in which the reinforcing bars were removed replicate rebar layouts that can be found in practice in structures from previous decades. The latter layouts would no longer comply with current design codes and standards and hence no design load can be specified for these specimens. The different reinforcement layouts are also shown in Figure 1.

3. Strut-and-tie models adopted

The selection of STMs for a structural assessment follows a common design practice. Such a selection is constrained by the reinforcement layout. Ties are taken to be parallel to the reinforcement, whereas struts may be inclined at any angle selected by the assessor, although typically the inclination will not be far outside the code specified limits. The assessor does, however, have some discretion in the number of reinforcement bars allocated to each tie. As there may be a number of STMs that satisfy the above requirements, the most suitable STM for a particular structure is that exhibiting the highest load-carrying capacity [1].

On the basis of the above, the STMs considered herein to provide a realistic description of the ULS function of the beams with the reinforcement layout indicated in Figure 1, are shown in Figure 2. The figure also shows, in light grey colour, the outline and reinforcement details of the beams. It is important to note that when tie and reinforcement directions coincide, only that particular reinforcement contributes to the formation of the tie. Such is the case of ties T1, T2, T3, T5 and T6 in Figure 2a, T1 and T2 in Figure 2b, T1, T4 and T5 in Figure 2c and T1, T2, T3, T4, T5 T6 and T7 in Figure 2d. Also, when a tie is shown to form in between two successive reinforcement bars, then, only these bars contribute to the formation of the tie. Such is the case of ties T4 in Figure 2a, and T2 and T3 in Figure 2c.

The STMs have been constructed so as to ensure the transfer of the applied load to the supports without violating the equilibrium conditions of the STM nodes. The failure load of the beams selected in the present work for the structural assessment is determined by the weakest individual element (relative to the calculated force to be resisted) of the STM. As discussed later, the STMs adopted in [7] for the structural assessment of beams NS-REF, NS-NU and NS-ND are also used in the present work for purposes of comparison. These models are shown in Figure 3.

4. Structural assessment

4.1. Beam NS-REF

The STM adopted for describing the function of beam NS-REF at ULS is shown in Figure 2a. The figure shows the portion of the beam between the cross section where the load is applied and the left-hand side support. The applied load V, the support reaction $R\,(=V)$, and the horizontal couple of internal forces F developing on account of bending at the cross section through the load point are also shown in the figure.

Calculating the strength of the struts (designated as S1 to S6 in Figure 2a) in accordance with current code provisions (e.g. [2]) produces values significantly larger than those corresponding to flexural capacity. Since the latter is attained at a load V_f over 40 % larger than its experimentally-established counterpart V_{EXP} = 402 kN, a strut failure cannot be the cause of loss of load-carrying capacity. For example, the strength of strut S3 calculated through the use of equation (6.5) in [2] is 737 kN, whereas, as will be seen later, the force developing under the experimentally-established load-carrying capacity $V_{EXP} = 402$ kN is only 354 kN. Therefore, a strut failure cannot be the cause of loss of load-carrying capacity. The latter can only occur due to a failure of the weaker (relative to the force to be resisted) of the ties designated as T1 to T6 in Figure 2a.

From Figure 2a, it can be seen that V is initially transferred along a single path comprising the STM members S6, T4 and S5. At the lower end of S5, this path bifurcates along T3 and T2, the latter transferring portions of V equal to xV and $(1-x)V$, respectively, from their lower to their upper end, with x being calculated as discussed later. Thereafter, the two portions of V are transferred to the support via struts S3 and S1.

The values of the forces developing in the STM members when the beam attains its experimentally-established load-carrying capacity $V_{EXP} = 402$ kN are calculated as follows:

(1.) From the moment equilibrium condition of the portion of the beam in Figure 2a, $F = 993.92$ kN,

(2.) Making use of the geometric characteristics of the STM, also indicated in Figure 2a, and considering the equilibrium conditions of the STM nodes yields the forces developing in the STM members as functions of x, with $x = 0.371$ being obtained by considering the equilibrium of the horizontal components of the forces acting on the STM node where members S2, S3, T3 and S4 meet,

(3.) With x already known, the forces developing in the struts and ties can be easily obtained from the equilibrium conditions of the STM nodes; they are as follows: $F_{S1} = 252.86$ kN, $F_{S2} = 544.22$ kN, $F_{S3} = 354.23$ kN, $F_{S4} = 544.44$ kN, $F_{S5} = 514.58$ kN, $F_{S6} = 603{,}02$ kN, $F_{T1} = 321.23$ kN, $F_{T2} = 337.15$ kN, $F_{T3} = 149.14$ kN, $F_{T4} = 402$ kN,

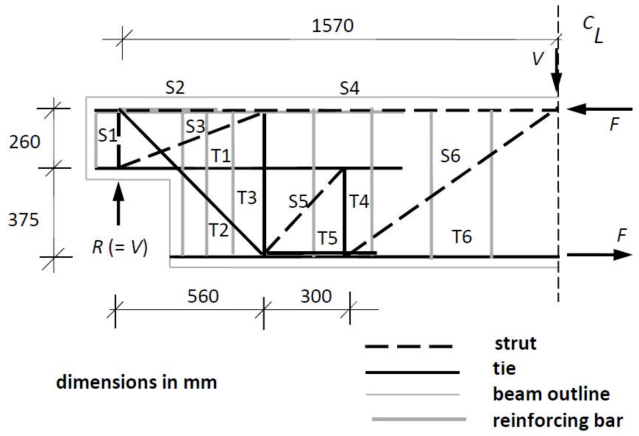

(A).

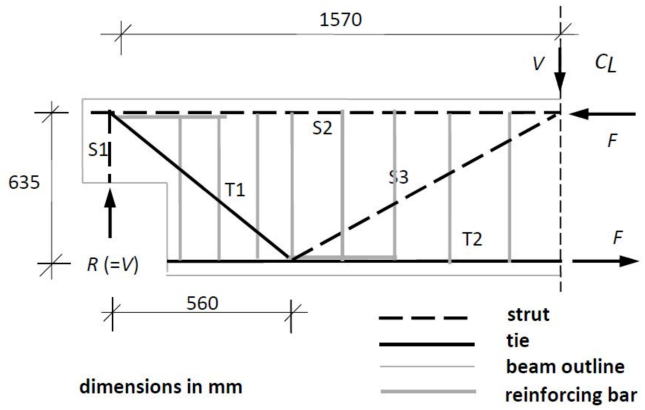

(B).

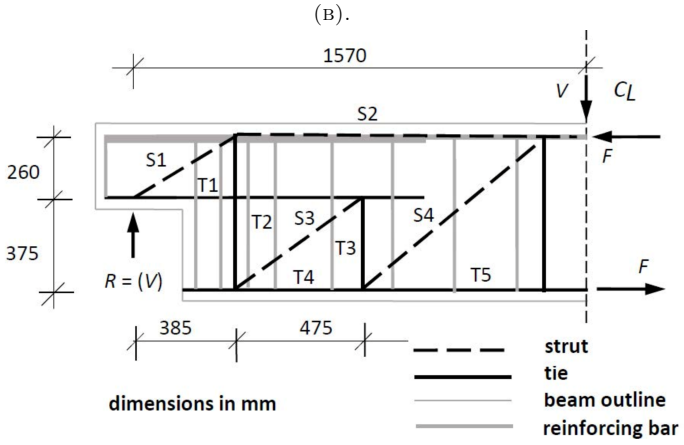

(C).

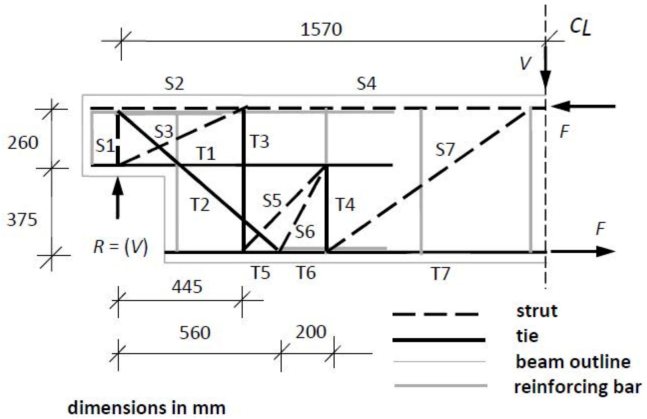

(D).

FIGURE 2. STMs of the beams with the different reinforcement layouts in Figure 1: (A) NS-REF, (B) NS-NU, (C) NS-ND, and (D) NS-RS.

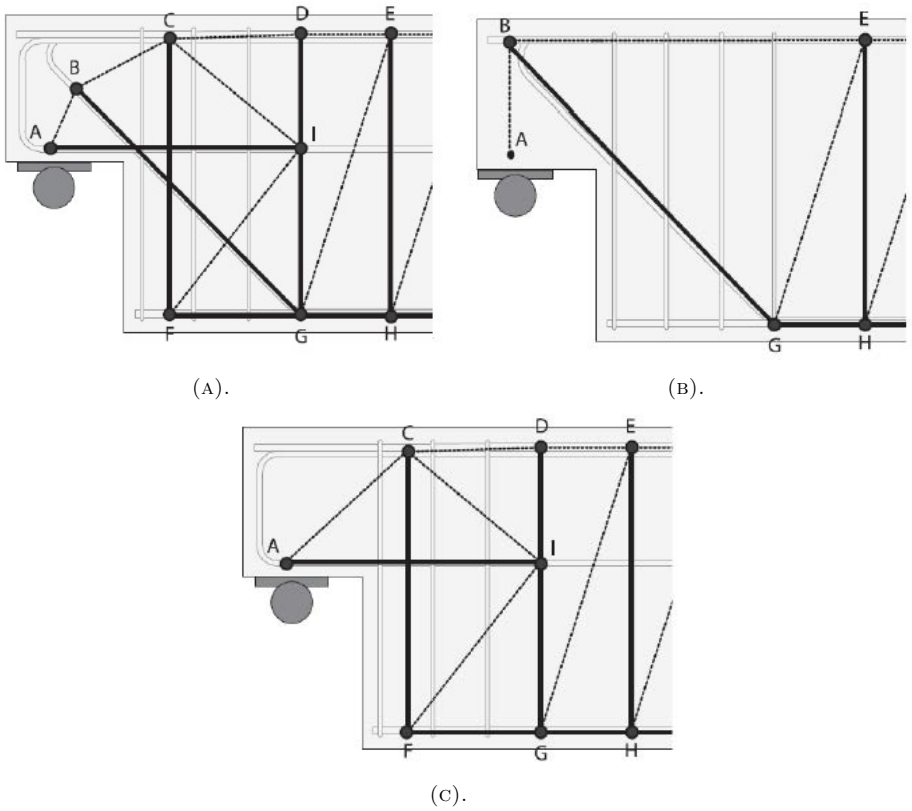

FIGURE 3. STMs adopted in Desnerck et al. [7] for beams: (A) NS-REF, (B) NS-NU, and (C) NS-ND.

$F_{T5} = 544.44\,\text{kN}$, and $F_{T6} = 993.92\,\text{kN}$, where F_{Si} and F_{Ti} with $i = 1$ to 6, are the forces developing at the struts and ties, respectively.

The strength of each tie depends on the number of reinforcing bars considered to contribute to its formation. As discussed in Section 3, the horizontal and diagonal ties comprise all available bars aligned in the direction and level of the ties, whereas, of the vertical ties, Figure 2a shows that only one two-legged 10 mm diameter link contributes to the formation of T3 and two three-legged 10 mm diameter links to the formation of T4.

The values of strength of the ties (obtained as the product of the cross-sectional area of the ties and the yield stress of the steel) together with the values of the forces expected to develop in the ties when the experimentally-established value of load-carrying capacity of beam NS-REF is attained (see item iii above) are provided in Table 1, which also includes the number of reinforcing bars forming each tie and the values of the yield stress of the reinforcing bars. From the table, it can be seen that the loss of load-carrying capacity is predicted to be controlled by a failure of tie T1 (weakest element relative to the calculated force to be resisted) comprising the U-bars of the nib reinforcement, with failure of the tie occurring at a load of about 56 % of the experimentally established peak load.

The alternative STM of beam NS-REF adopted by [7] is shown in Figure 3a, with the forces developing in the ties AI, BG, CF, IG and EH at the experimentally-established peak load being given in Table 2. The table also includes the number of reinforcing bars forming each tie, the yield stress of the bars together with the resulting strength of the ties. From the table, it can be seen that the tie controlling the failure of the STM is tie EH, which is predicted to fail at a load of about 31 % of the experimentally-established value; this value is significantly smaller than the 56 % predicted by the STM adopted in the present work. Since STMs are developed within the context of the lower-bound theory of plasticity [1], the proposed model is considered more preferable for a structural assessment than the model proposed in [7].

4.2. BEAM NS-NU

The STM of the beam at ULS is shown in Figure 2b. The internal forces F developing on account of bending at the mid-span cut are found equal to 731.84 kN by considering (as for beam NS-REF) the moment equilibrium condition of the beam when it reaches its experimentally-established load-carrying capacity $V_{EXP} = 296\,\text{kN}$. By solving the equations of equilibrium of the STM nodes it is found that the forces developing in the STM members are $F_{S1} = 296\,\text{kN}$, $F_{S2} = 261.04\,\text{kN}$, $F_{S3} = 556.12\,\text{kN}$, $F_{T1} = 394.66\,\text{kN}$, and $F_{T2} = 731.84\,\text{kN}$.

Ties	Number of bars	Cross-sectional area of tie [mm^2]	Yield stress f_y [MPa] of reinforcement	Calculated Value strength F_u [kN] of tie	Forces in ties at experimental load-carrying capacity F_{EXP} [kN]	F_u/F_{EXP}
T1	3D12	339.29	529	179.49	321.23	0.56
T2	4D12	452.39	529	239.15	337.15	0.69
T3	2D10	157.08	539	84.67	149.14	0.57
T4	2×3D10	471.24	539	253.00	402.00	0.63
T5	5D25	2454.37	578	1418.43	544.44	2.61
T6	5D25	2454.37	578	1418.43	993.92	1.43

TABLE 1. Ties' strength and forces developing in the ties of the STM of beam NS-REF at the experimentally-established load-carrying capacity $V_{EXP} = 402\,\text{kN}$.

Ties	Number of bars	Cross-sectional area of tie [mm^2]	Yield stress f_y [MPa] of reinforcement	Calculated Value strength F_u [kN] of tie	Forces in ties at experimental load-carrying capacity F_{EXP} [kN]	F_u/F_{EXP}
AI	3D12	339.29	529	179.49	216.46	0.83
BG	4D12	452.39	529	239.15	220.51	1.08
CF	2×2D10	314.16	539	169.33	243.85	0.69
IG	2×D10	157.08	539	84.67	243.85	0.35
EH	3×D10	235.62	539	127.00	402.00	0.31

TABLE 2. Ties' strength and forces developing in the ties of the STM adopted in [7] for beam NS-REF at the experimentally-established load-carrying capacity $V_{EXP} = 402\,\text{kN}$.

Failure can only be linked with a failure of the inclined tie, T1, since, as for the STM of beam NS-REF, the load-carrying capacity of the struts calculated in accordance with [2], is found significantly larger than the value corresponding to the experimentally-established failure load of the beams; also, the large cross-sectional area of tie T2 (comprising five 25 mm diameter bars) precludes failure of the tie under the load that caused the failure of the beam. The strength of T1 (comprising four 12 mm diameter bars with a total cross-sectional area of 452.39 mm^2 and a yield stress of 529 MPa) is $F_u = 231.31\,\text{kN}$, whereas the force expected to develop in the tie when the beam attains its experimentally-established load-carrying capacity F_{EXP} was found, as discussed earlier, to be $F_{T1} = 394.66\,\text{kN}$, i.e. $F_{EXP} = F_{T1}$. Therefore, $F_u/F_{EXP} = 0.61$.

The alternative STM of beam NS-NU adopted in [7] is shown in Figure 3b. From the conditions of equilibrium of nodes B, G and E, it is easily established that the forces developing in ties BG and EH at the experimentally-established peak load of 296 kN are $F_{BG}^{EXP} = 394.66\,\text{kN}$ and $F_{EH}^{EXP} = 296\,\text{kN}$. As ties BG and EH comprise four 12 mm diameter bars with a yield stress of 529 MPa and three 10 mm diameter bars with a yield stress of 539 MPa, respectively, the forces that they carry at yield are $F_{BG}^{STM} = 231.31\,\text{kN}$ and $F_{EH}^{STM} = 68.18\,\text{kN}$, which are about 61 % and 23 %, respectively, of the values of F_{BG}^{EXP} and F_{EH}^{EXP}, i.e. $F_{BG}^{STM}/F_{BG}^{EXP} = 0.61$ and $F_{EH}^{STM}/F_{EH}^{EXP} = 0.23$. Therefore, tie EH controls the failure and, on the basis of this, the STM of Figure 3b is predicted to fail at a load significantly lower than that of the STM adopted in the present work (see Figure 2b). Thus, as for the STM of beam NS-REF, the adopted model in the present work is found to be more suitable for the structural assessment than the STM adopted in [7].

4.3. BEAM NS-ND

The STM adopted for this beam at its ULS is shown in Figure 2c. As for beams NS-REF and NS-NU, the internal forces at the beam mid-span cut and the forces developing at the STM members are calculated from the equation of moment equilibrium of the beam and the equations of equilibrium of the STM nodes, respectively. They are found to be $F = 605.75\,\text{kN}$, $FS1 = 438.13\,\text{kN}$, $F_{S2} = 362.79\,\text{kN}$, $F_{S3} = 395.39\,\text{kN}$, $F_{S4} = 345\,\text{kN}$, $F_{T1} = 362.79\,\text{kN}$, $F_{T2} = 245\,\text{kN}$, $F_{T3} = 245\,\text{kN}$, $F_{T4} = 362.79\,\text{kN}$, and $F_{T5} = 605.75\,\text{kN}$.

As for beams NS-REF and NS-NU, the STM struts and the ties comprising five 25 mm diameter bars have a strength significantly larger than the forces developing in these STM members when the experimentally-established value of the failure load $V_{EXP} = 245\,\text{kN}$

Ties	Number of bars	Cross-sectional area of tie [mm^2]	Yield stress f_y [MPa] of reinforcement	Calculated Value strength F_u [kN] of tie	Forces in ties at experimental load-carrying capacity F_{EXP} [kN]	F_u/F_{EXP}
T1	3D12	339.29	529	179.49	362.79	0.49
T2	2×2D12	314.16	529	169.33	245.00	0.69
T3	2×3D10	471.24	539	254.00	245.00	1.04

TABLE 3. Ties' strength and forces developing in the ties of the STM of beam NS-ND at the experimentally-established load-carrying capacity $V_{EXP} = 245\,\text{kN}$.

Ties	Number of bars	Cross-sectional area of tie [mm^2]	Yield stress f_y [MPa] of reinforcement	Calculated Value strength F_u [kN] of tie	Forces in ties at experimental load-carrying capacity F_{EXP} [kN]	F_u/F_{EXP}
T1	3D12	339.29	529	179.49	233.49	0.77
T2	4D12	452.39	529	239.15	296.77	0.81
T3	2D10	157.08	539	84.67	136.47	0.62
T4	3D10	235.62	539	127.00	359.00	0.35

TABLE 4. Ties' strength and forces developing in the ties of the STM of beam NS-RS at the experimentally-established load-carrying capacity $V_{EXP} = 359\,\text{kN}$.

is attained. Therefore, failure of the STM can only occur due to a failure of the weakest of ties T1, T2 and T3 relative to the force expected to develop when the beam's V_{EXP} is attained. The values of strength and the values of the forces developing in these ties when the applied load reaches the value of V_{EXP} are shown in Table 3 together with the number of the steel bars comprising each tie and the yield stress of the bars. From the table, it can be seen that the tie controlling the loss of load-carrying capacity of the adopted STM is tie T1, which fails at a load of about 49 % of the experimentally-established peak value of beam NS-ND.

The alternative STM of beam NS-ND adopted in [7] is shown in Figure 3c. From the figure, it is apparent that the tie controlling failure of the STM is tie IG which comprises two 10 mm diameter bars with a yield stress of 539 MPa and, therefore, can carry a force $F_{IG}^{STM} = 2 \cdot (\pi \cdot 10^2/4) \cdot 539 = 84.67\,\text{kN}$. Since the force that would develop in this tie, had it been possible for the STM to sustain the experimentally-established peak load of 245 kN, is $F_{IG}^{EXP} = 245\,\text{kN}$, the STM's load-carrying capacity is only $F_{IG}^{STM}/F_{IG}^{EXP} = 84.67/245 \approx 0.35 = 35\,\%$ that of the beam tested. The latter value is significantly smaller than the value of 49 % obtained for the STM adopted in the present work, which, yet again, is found to be a more suitable model for the structural assessment.

4.4. BEAM NS-RS

The STM adopted for beam NS-RS at its ULS is shown in Figure 2d. As for beam NS-REF, the load transfer is initially accomplished along a single path which, later on, bifurcates and, eventually, the applied load reaches the support via struts S1 and S3. The forces developing in the STM members when the beam reaches the experimentally established failure load $V_{EXP} = 359\,\text{kN}$ are calculated as for beam NS-REF and found to be: $F_{S1} = 228.58\,\text{kN}$, $F_{S2} = 196.29\,\text{kN}$, $F_{S3} = 310.51\,\text{kN}$, $F_{S4} = 429.07\,\text{kN}$, $F_{S5} = 178.19\,\text{kN}$, $F_{S6} = 882.87\,\text{kN}$, $F_{S7} = 581.88\,\text{kN}$, $F_{T1} = 233.49\,\text{kN}$, $F_{T2} = 296.77\,\text{kN}$, $F_{T3} = 136.42\,\text{kN}$, $F_{T4} = 359\,\text{kN}$, $F_{T5} = 929.67\,\text{kN}$, and $F_{T6} = 887.61\,\text{kN}$.

For the reasons discussed in the preceding section, the STM struts and the ties comprising five 25 mm diameter bars are unlikely to fail before the applied load reaches its experimentally-established peak value. Therefore, failure of the STM can only occur due to a failure of the weakest of T1, T2, T3 and T4 relative to the force expected to develop when the applied load attains its experimental peak value of 359 kN.

The values of strength and the values of the forces developing in the above ties at peak load are shown in Table 4 together with the number of the bars comprising each tie and the yield stress of the steel bars. From the table, it can be seen that the tie controlling the failure of the STM is tie T4, which yields at a value of the applied load of about 35 % of the experimentally-established value of the peak load of the beam.

5. Discussion

From the results presented in the preceding section, it is seen that the STMs adopted for the beams tested predict values of load-carrying capacity that underestimate their experimentally-established counterparts by a margin which varies between approximately 40 % and 65 %.

More specifically, for beam NS-REF, the load-carrying capacity is underestimated by about 44 % with the weakest tie of the STM being the longitudinal tie T1, which, as indicated in Figure 2a, extends between the node at the beam support and the node where T1 intersects with S5 and T4. Therefore, the STM, by its nature, predicts that failure may initiate at any point along the length of T1. However, the experiment established that failure was preceded by yielding and/or rupture, in the region of the re-entrant corner, of not only the three 12 mm diameter U bars comprising tie T1, but also the four 12 mm diameter diagonal bars comprising tie T2 and the two-legged 10 mm diameter link closest to the re-entrant corner; moreover, the specimen suffered horizontal splitting of concrete in the compressive zone in the region of the nib (see Figure 4) [5].

The STM of beam NS-NU was found to exhibit a load-carrying capacity of 61 % of the value of its counterpart established from the tests. However, as for beam NS-REF, the STM predicts that failure may occur anywhere along the length of the weakest tie which is T1 (see Figure 2b) and the test results indicate that the loss of load-carrying capacity is preceded by yielding, in the region of the re-entrant corner, of not only the four 12 mm diameter diagonal bars comprising T1, but also yielding of the two-legged 10 mm diameter stirrup nearest to the re-entrant corner, as well as horizontal splitting of concrete in the compressive zone in the region of the nib (see Figure 4) [5].

Similar predictions were obtained for beam NS-ND. The loss of load-carrying capacity was linked with tie T1 (see Figure 2c that was found to be the weakest tie (see Table 2) with the experimental results showing that the failure of the beam is preceded by yielding, in the region of the re-entrant corner, of not only the three 12 mm diameter U-bars comprising T1, but also the two-legged 10 mm diameter stirrup closest to the re-entrant corner, as well as horizontal splitting of concrete in the compressive zone in the region of the nib as for beams NS-REF and NS-NU (see Figure 4). However, yet again, the predicted load-carrying capacity was less than half the experimentally-established value (see Table 3).

It should be noted at this stage that predicting failure of the longitudinal and diagonal ties precludes the likelihood of improvement of the STM predicted value of load-carrying capacity through an alternative STM with transverse ties comprising a larger number of links. Moreover, from the experimental results presented in [5], failure of the beam discussed above appears to be linked with flexural failure of the beams' cross section that includes the inclined crack that invariably forms at the re-entrant corner (at an angle of about 45o with respect to the longitudinal axis) and penetrates deeply into the compressive zone. Assuming that the Bernoulli assumption is sufficiently accurate for practical purposes, the calculation of flexural capacity is rather straightforward by considering the conditions of equilibrium of the internal forces developing in concrete of the compressive zone and the reinforcing bars crossing the inclined crack as indicated in Figure 5. In the figure, $F_{c,c}$ is the force sustained by concrete in the compressive zone, $F_{s,c}$ the force sustained by the longitudinal steel reinforcement of the compressive zone, $F_{s,v}$ the force sustained by the vertical steel reinforcement crossing the inclined crack, $F_{s,u}$ the resultant of the forces developing in the U-bars in the region of the re-entrant corner and $F_{s,Dh}$ and $F_{s,Dv}$ the horizontal and vertical components of the resultant of the forces developing in the diagonal bars.

After the calculation of flexural capacity in accordance with current code methods, the solution of the equation of moment equilibrium of the portion of the beam between the cross section considered and the support results in the following values of load-carrying capacity: $R_{f,REF} = 352\,\text{kN}$, $R_{f,ND} = 170\,\text{kN}$, $R_{f,NU} = 261\,\text{kN}$, for beams NS-REF, NS-ND and NS-NU, respectively. Thus, the corresponding ratios of the calculated to the experimental values are 0.88, 0.7 and 0.88, respectively. Moreover, a flexural type of failure is consistent with both the horizontal splitting of concrete in the compressive zone of the cross section and the yielding/rupture of the reinforcement crossing the inclined crack, as observed in the experiment. This is a significantly improved prediction of load-carrying capacity indicative of the advantages that may stem from adopting, as the basis for structural assessment, the modified beam theory first proposed in [8] and described in more detail in [9] and [10].

As regards beam NS-RS, not only the deviation of the predicted value of load-carrying capacity from its experimentally-established counterpart was significantly larger than that of beams NS-REF, NS-NU and NS-ND – the predicted value was merely 35 % of that established experimentally – but also the predicted location of failure differed from that established by experiment. The failure was predicted to occur due to failure of the lower end of the links forming tie T4 (see Figure 2d), whereas the loss of load-carrying capacity was found, by experiment, to occur due to horizontal splitting of concrete in the region of the beam between the tips of the deep inclined cracks in the full depth region and the upper face of the beam (see Figure 4). In accordance with the work presented in [9] and Kotsovos [10] such horizontal splitting of the compressive zone is caused by the action of transverse tensile stresses that develop for purposes of transverse deformation compatibility that is not allowed for in strut-and-tie modelling.

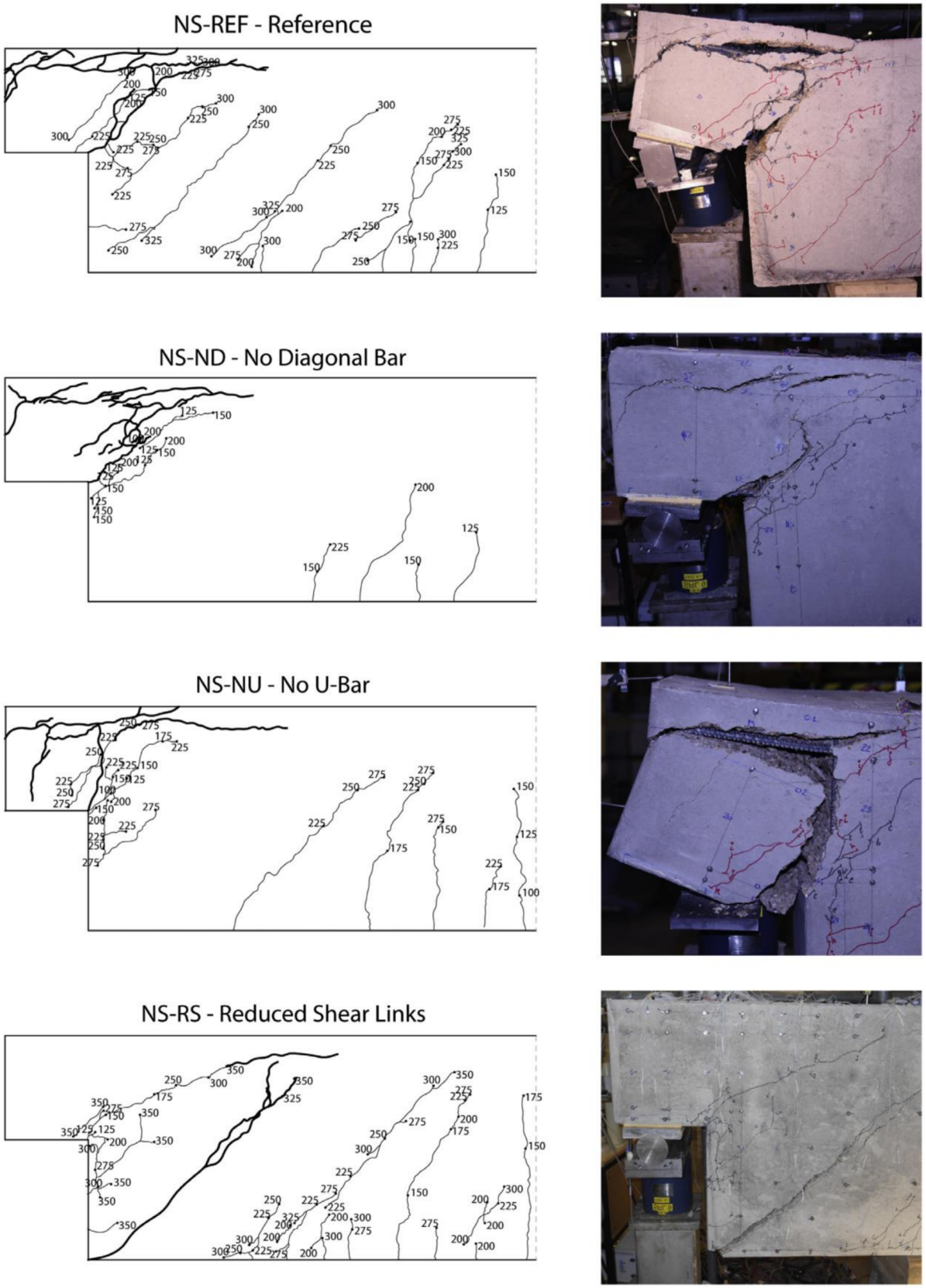

FIGURE 4. Final crack pattern of tested RC half-joint beams tested by Desnerck et al. [5].

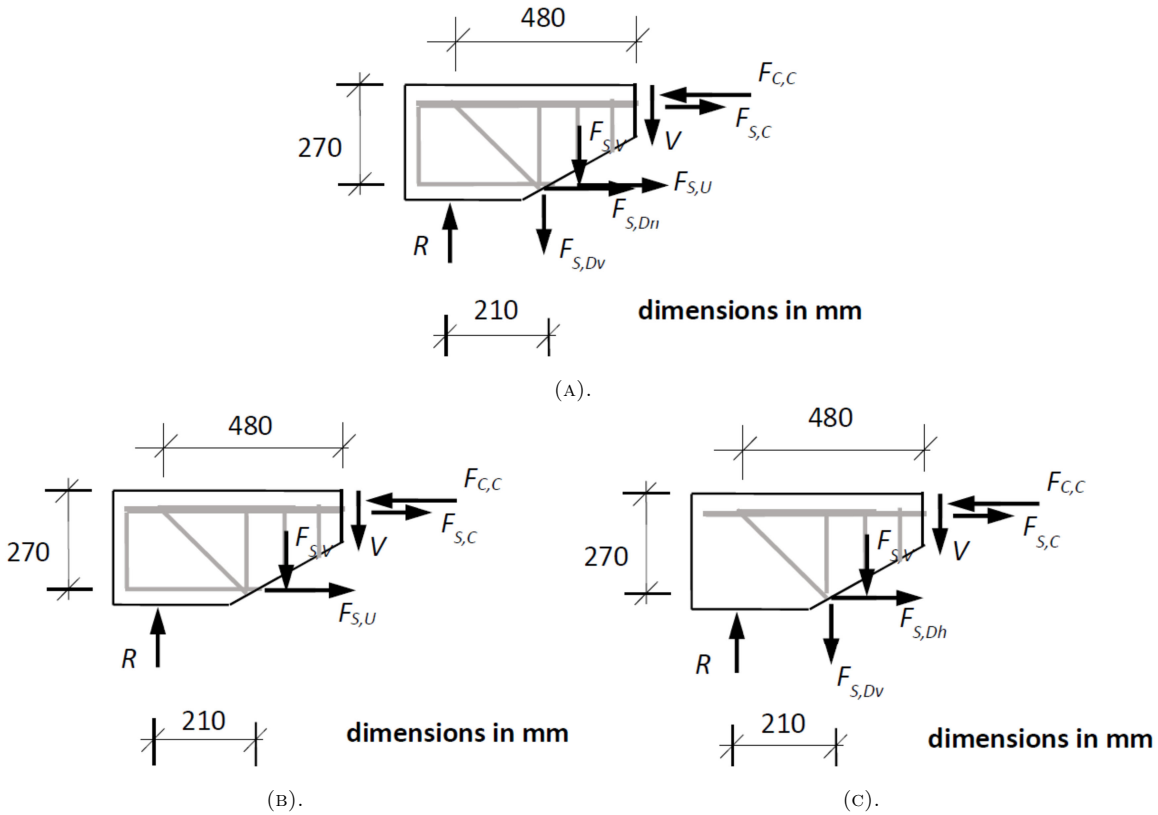

FIGURE 5. Internal forces in cross section including diagonal crack at re-entrant corner of beam (A) NS-REF, (B) NS-ND, and (C) NS-NU.

It appears from the above, therefore, that the use of STM for the structural assessment of half-jointed beams has two significant drawbacks not recognized until now: it underestimates load-carrying capacity by a factor larger than two, and, even when the causes of failure are correctly identified, cannot predict the location of the failure. Thus, there is a need for an alternative design method, the development of which could be based on concepts such as those presented in [8–10], capable of realistically describing both structural-concrete behaviour and the causes of failure underlying the loss of load-carrying capacity.

6. CONCLUSIONS

From the work presented in the paper, the following conclusions may be drawn:

In all cases considered, the predicted values of load-carrying capacity are significantly smaller than widely expected from their experimentally-established counterparts. The deviation of the predicted from the measured values ranges between 40 % and 65 %.

Moreover, they are found unable to predict the location of failure.

More specifically, strut-and-tie modelling is found unable to predict strut failure due to horizontal splitting of concrete in the compressive zone, which characterises the mode of failure of the beams tested. For beams NS-REF, NS-NU and NS-ND, such splitting occurred in the region of the nib, whereas for beam NS-RS, in the full-depth region at a distance nearly equal to the cross-sectional depth from the re-entrant corner.

By nature, strut-and-tide models can only predict yielding and/or rupture of the reinforcement that comprises the tie controlling the failure of the model. For beams NS-REF, NS-NU and NS-ND, the tie predicted to control the failure consisted of reinforcing bars which did, in fact, yield before the loss of load-carrying capacity of the beams tested. However, as yielding can occur anywhere along the length of the tie, the location of the yielding of the reinforcement comprising this tie cannot be identified by the strut-and-tie model alone.

As regards beam NS-RS, the vertical tie predicted to control the failure is in the region of the applied load and not near the nib were the stirrups were found experimentally to yield before loss of load-carrying capacity of the specimen tested. Yet, failure was suffered due to horizontal splitting of concrete in the compressive zone of the full-depth region of the beam, which the model failed to predict.

In view of the above, there is a need for an alternative assessment method based on concepts capable of both realistically describing structural-concrete behaviour and identifying the causes of failure leading to loss of load-carrying capacity.

List of symbols

F Internal forces developing on account of bending

$F_{C,C}$ Force sustained by concrete in the compressive zone

F_{EXP} Force developing at the weakest tie when $V = V_{EXP}$

$F_{S,C}$ Force sustained by compression reinforcement

$F_{S,V}$ Force sustained by links crossing inclined crack at re-entrant corner

$F_{S,Dh}$, $F_{S,Dv}$ Horizontal and vertical components of force sustained by the diagonal reinforcement in a region of re-entrant corner

$F_{S,U}$ Force sustained by U-bars in a region of re-entrant corner

F_{S1} to F_{S7} Forces developing in the struts of STM

F_{T1} to F_{T7} Forces developing in the ties of STM

F_u Calculated force developing in the weakest tie

R Reaction at support

V Applied load

V_{EXP} Experimentally established load-carrying capacity

V_f Load at flexural capacity

$V_{f,REF}$, $V_{f,ND}$, $V_{f,NU}$ Load at flexural capacity of cross section including inclined crack at re-entrant corner of beams NS-REF, NS-ND and NS-NU, respectively

Half-joint beams assessed

NS-REF Reference specimen

NS-ND Specimen without diagonal reinforcement, but, in all other aspects, with reinforcement layout identical to that of NS-REF

NS-NU Specimen without u-bar reinforcement, but, in all other aspects, with reinforcement layout identical to that of NS-REF

NS-RS Specimen with reinforcement layout identical to that of NS-REF, but with a reduced number of stirrups

References

[1] J. Schlaich, K. Schafer, M. Jennewein. Toward a consistent design of structural concrete. *PCI Journal* **32**(3):74–150, 1987. https://doi.org/10.15554/pcij.05011987.74.150.

[2] The European Committee for Standardization. Eurocode 2: Design of concrete structures. Part 1-1: General rules and rules for buildings. (Standard No. EN 1992-1), 2004.

[3] The European Committee for Standardization. Eurocode 8: Design of structures for earthquake resistance. Part 1-1: General rules, seismic standards and rules for buildings. (Standard No. EN 1998-1), 2004.

[4] Transport Scontland (Agency of the Scottish Executive). TS interim amendment N°20 – Concrete half-joint deck structures, 2006. [2022-10-15], https://www.transport.gov.scot/media/6084/ts_ia_20.pdf.

[5] P. Desnerck, J. M. Lees, C. T. Morley. Impact of the reinforcement layout on the load capacity of reinforced concrete half-joints. *Engineering Structures* **127**:227–239, 2016. https://doi.org/10.1016/j.engstruct.2016.08.061.

[6] FIB Task Group 4.4. FIB bulletin 45 – Practitioners' guide to finite element modelling of reinforced concrete structures, 2011. International Federation for Structural Concrete.

[7] P. Desnerck, J. M. Lees, C. T. Morley. Strut-and-tie models for deteriorated reinforced concrete half-joints. *Engineering Structures* **161**:41–54, 2018. https://doi.org/10.1016/j.engstruct.2018.01.013.

[8] M. D. Kotsovos. *Compressive Force-Path Method: Unified Ultimate Limit-State Design of Concrete Structures*. Springer, London, 2014.

[9] M. D. Kotsovos. Conflicts between reinforced concrete design assumptions and actual concrete behaviour. *Proceedings of the Institution of Civil Engineers – Structures and Buildings* **175**(1):34–45, 2022. https://doi.org/10.1680/jstbu.19.00003.

[10] M. D. Kotsovos. Beam theory – A proposed alternative basis for RC design. *Proceedings of the Institution of Civil Engineers – Structures and Buildings* 2021. [Ahead of print], https://doi.org/10.1680/jstbu.20.00064.